

---

# Nonstationary image processing via Gabor transforms

Michael P. Lamoureux and Daniel H. Adler

## ABSTRACT

We illustrate some of the key ideas of nonstationary filter and Gabor deconvolution via a simple application of Gabor transforms to standard image processing.

## INTRODUCTION

Seismic signals are nonstationary – that is, their characteristic changes over the length of a recording, reflecting the fact that the seismic wave is altered as it propagates through various geological layers of the earth. Some familiar alterations include attenuation due to spherical spreading, frequency-shaping due to  $Q$ -effects, and amplitude variations due to inhomogeneous reflectivity. Thus, it is fundamental in seismic data processing to have techniques which take into account the nonstationary nature of the signal. Processors are interested in developing algorithms for nonstationary filtering, nonstationary deconvolution, and other methods which modify a signal in a time-varying manner.

One key approach to developing such algorithms depends on the use of the Gabor transform, which is a time-frequency method based on a localized version of the Fourier transform. Denis Gabor, inventor of the hologram, proposed analyzing signals as a sum of modulated Gaussian functions. This idea has been extensively developed by the signal processing community (see, for instance, Feichtinger and Strohmer (1998)) and recently applied to problems in seismic imaging. For instance, a powerful extension to Wiener deconvolution based on the Gabor transform has been proposed and implemented by Margrave et al. (2002). Similarly, novel algorithms for estimating  $Q$  attenuation in time-frequency domain have been developed by Grossman et al. (2002). More recently, wavefield extrapolation based on the use of Gabor multipliers have been implemented.

However, a basic problem we run into when developing Gabor methods for seismic imaging, or trying to explain them to new users, is that we are trying to understand a complex mathematical technique which is being applied to very complex, real data signals. That is, the seismic data is very rich in complex physical phenomena, and it takes a high level of sophistication simply to understand what the data represents, even before we get the mathematics underway. The situation would be greatly simplified if we could develop the mathematical ideas on a simpler set of data. Hence this article – we show how Gabor transform techniques can be applied to simple sounds, and photographic images, which will give a basic understanding of these methods before applying them to the seismic problems.

## THE GABOR TRANSFORM

The Gabor transform is a localized version of the Fourier transform that provides local frequency information about a given signal. It is typically computed by applying a sliding window function  $w_\tau(t) = w(t - \tau)$  to the signal  $s(t)$ , taking the product, and extracting the local frequency information by taking the Fourier transform of this product. The Gabor

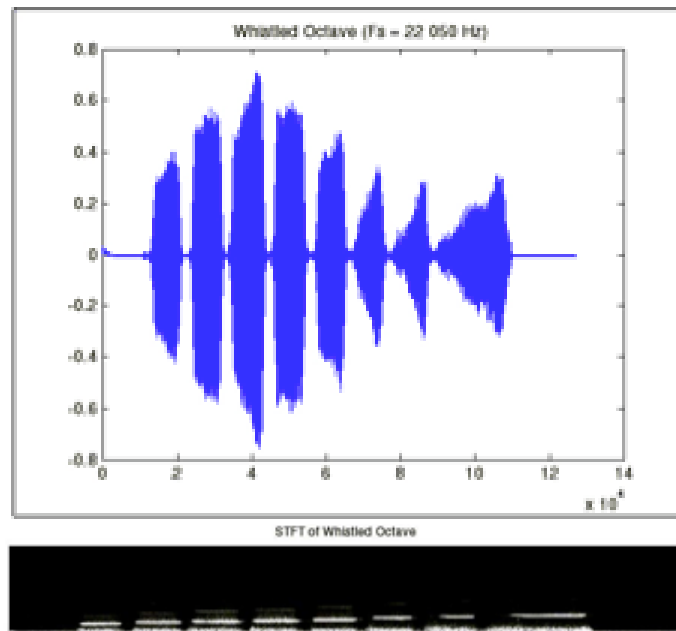


FIG. 1. A whistled tune, and its Gabor transform.

transform of signal  $s$ , evaluated at time  $\tau$ , frequency  $\omega$ , is thus

$$G(\tau, \omega) = FFT\{w_\tau(\cdot)s(\cdot)\}(\omega). \quad (1)$$

Without worrying too much about the details of this transform, we see immediately that the result  $G(\tau, \omega)$  is a function of both time  $\tau$  and frequency  $\omega$ , and ideally should represent local frequency information about the signal. As an illustration, we compute the Gabor transform of a recording of a person whistling a tune, as shown in Figure 1. The time-frequency representation (in the bottom half of the figure) clearly shows the notes localized in time, with a general upward trend in the frequency of the notes.

Similarly, a recording of ToneTone<sup>TM</sup> signals from a telephone can be decomposed by the Gabor transform, and the result in Figure 2 clearly shows each tone burst as a combination of two pure tones, at various frequencies.

The Gabor transform comes with an inverse; thus once the signal  $s(t)$  has been transformed to  $G(\tau, \omega)$ , it can be recovered exactly. Typically, the inverse is computed by applying an inverse Fourier transform to the Gabor function, applying a dual window  $w'(t)$  and summing over various translates of this window. That is, we recover the signal  $s(t)$  as

$$s(t) = \sum_j w'(t - \tau_j) IFFT(G(\tau_j, \omega)), \quad (2)$$

where the inverse FFT is applied in the  $\omega$  variable. It is important to correctly choose the dual window  $w'(t)$  and its spacing with the  $\tau_j$ . When this is done incorrectly, the exact inverse is not obtained. For instance, when the Gabor transform is applied in two dimensions to a test image as in Figure 3, there is an obvious problem in the reconstruction shown in Figure 4, where visual blocks appear. This was a particularly nice demonstration of how the use of real images, rather than seismic signals, highlighted an error in initial codes our student put together.

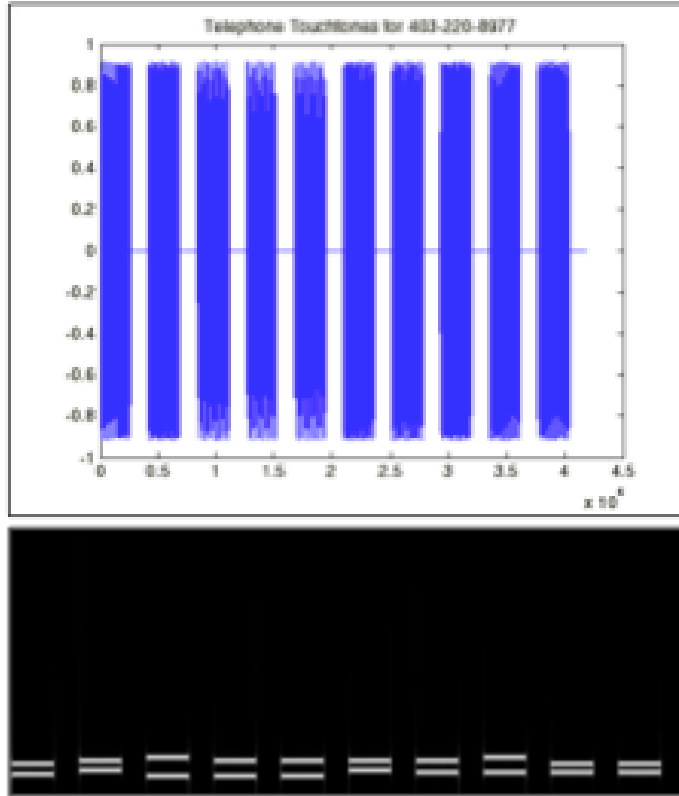


FIG. 2. TouchTone signals and their Gabor transform.

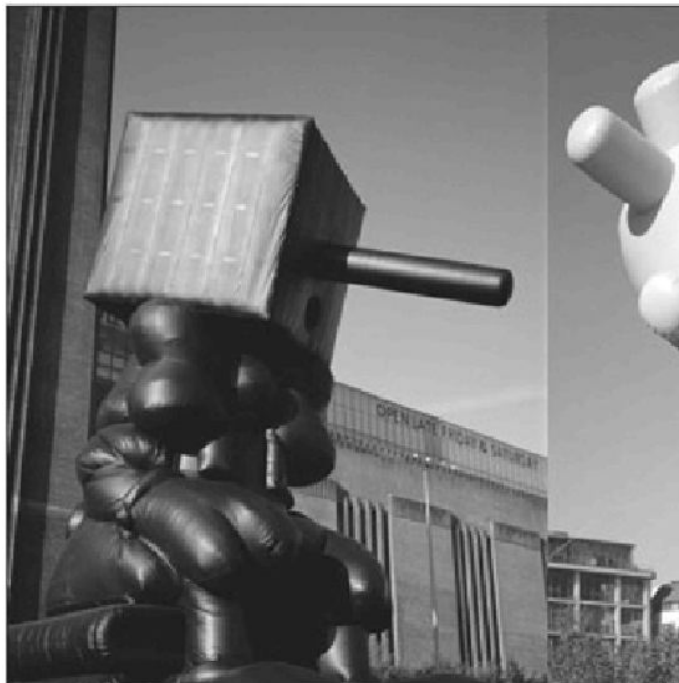


FIG. 3. A simple test image, before filtering.



FIG. 4. Reconstructed image, with improper windowing.

## Windows

A proper selection of window functions is important to ensure an exact inverse. The key connection between the window  $w(t)$ , its dual  $w'(t)$ , and their translates, is the partition of unity condition:

$$\sum_j w(t - \tau_j)w'(t - \tau_j) = 1. \quad (3)$$

That is, once we sum the products of the translates of the windows, the  $t$  dependence disappears and the functions add up to one.

Denis Gabor proposed using multidimensional Gaussians as the window functions,  $w(t) = e^{-t^2}$ , as shown in in Figure 5. However, no matter how one translates these, they do not sum to one exactly (although good approximations are possible). A better choice in two dimensions would be the product of two raised cosine functions,  $w(t) = (\cos(t_1) - 1)(\cos(t_2) - 1)$ , as shown in Figure 6. If we take nine of these windows, properly spaced, we see they sum to a constant plateau in the middle, as shown in Figure 7. Summing many such windows gives a flat plateau as large as necessary.

In these examples, the window function  $w(t)$  is carefully chosen so that the dual window can simply be taken as the constant one. The roles could be reversed, so  $w(t)$  is the constant one, and  $w'(t)$  is raised cosine window. A useful compromise which localizes both the Gabor transform and the reconstruction is to choose both  $w(t)$  and  $w'(t)$  to be the square root of the raised cosine window. Their product then forms the partition of unity.

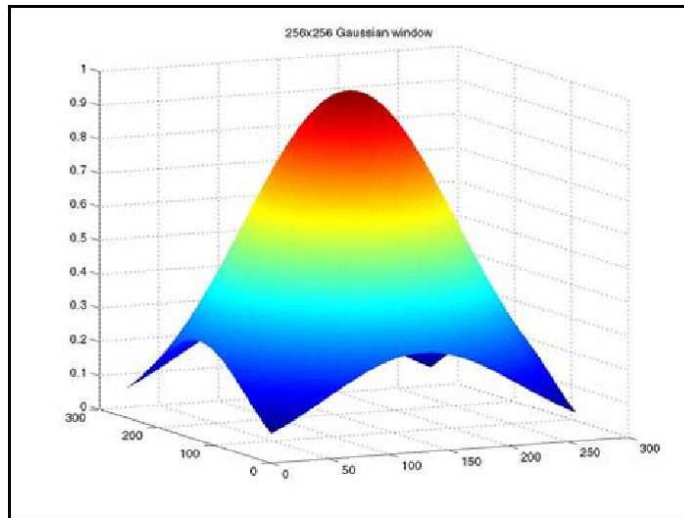


FIG. 5. A Gaussian window in 2D.

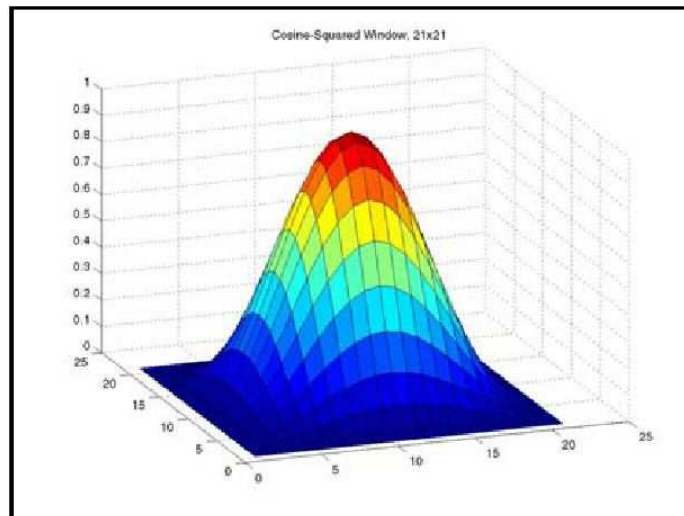


FIG. 6. A raised cosine window in 2D.

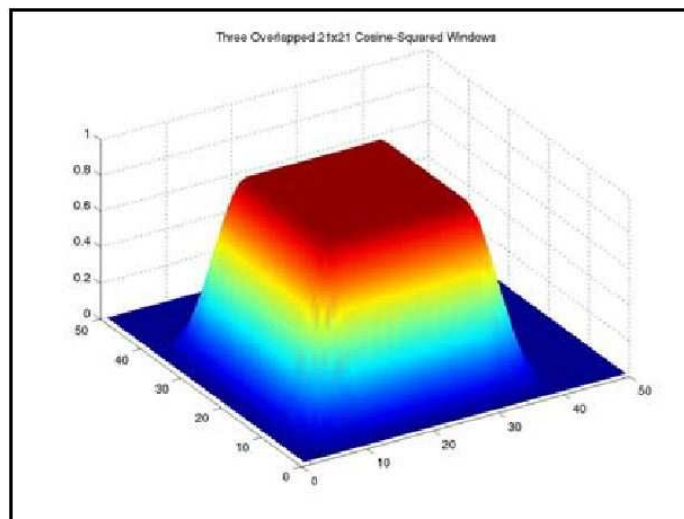


FIG. 7. Nine cosine windows sum to a flat plateau.

## NONSTATIONARY FILTERING

The key idea behind nonstationary filtering is to somehow apply different filters (or filters with different characteristics) to different parts of a signal. In a seismic signal, one may wish to perform different levels of whitening at different parts of the data, or design a deconvolution method that changes the frequency content of a signal by different amounts, at different times in the signal. Again, understanding the filtering process for seismic data assumes the student already understands a lot about the physics of the processes generating a seismic signal. Here, we want to simplify by working with images.

For nonstationary filtering of a photographic image, one might imagine blurring one part of an image, while simultaneously sharpening another part of the image. In the Fourier domain, blurring is achieved by suppressing the high (spacial) frequencies, while sharpening is achieved by suppressing the low frequencies. To do both simultaneously in the Gabor domain, one simply suppresses high or low frequencies in  $G(\tau, \omega)$  depending on the  $\tau$  variable. This is easily achieved by multiplying the Gabor function with some other function  $\alpha(\tau, \omega)$  that has necessary characteristics. The new, modified signal is obtained by applying the inverse Gabor transform, so

$$\tilde{s}(t) = \sum_j w'(t - \tau_j) IFFT\{\alpha(\tau_j, \omega) G(\tau_j, \omega)\}(t). \quad (4)$$

The function  $\alpha(\tau, \omega)$  creates a Gabor multiplier, which is a powerful technique for implementing nonstationary filters. Again, for photographic images, it is easy to see the effect of any particular Gabor multiplier. For instance, we can selectively filter our test image by blurring in one corner while sharpening in the opposite, with a smooth transition in between. Figure 8 is the result of this nonstationary filtering of the test image.

It is even possible to design the nonstationary filter “on the fly,” using interactive picks with a computer mouse to identify regions that should be selectively filtered. For instance, we can begin with the test image in Figure 9, pick out some spots to be blurred, others to be sharpened, and apply the resulting Gabor multiplier to obtain the edited image in Figure 10. One can clearly see the results of the localized blurring and sharpening. In this particular example, one also sees a darkening of the image at the sharpened zones – this is due to an error in the design of this particular multiplier, which again demonstrates how using familiar images in developing the Gabor methods can help quickly identify problems.

The precise specification of the Gabor multiplier  $\alpha(\tau, \omega)$  for use in seismic problems is a subject of considerable interest to our research team, and has been discussed in Gibson et al. (2003). However, for a simple task like photo imaging, simple choices for  $\alpha$  often work very well.

## CONCLUSIONS

We have demonstrated the use of the Gabor transform, a time-frequency method, in analysis of simple sounds and the nonstationary filtering of photographic images. These techniques have great utility in the processing of seismic data, but it is useful to develop an

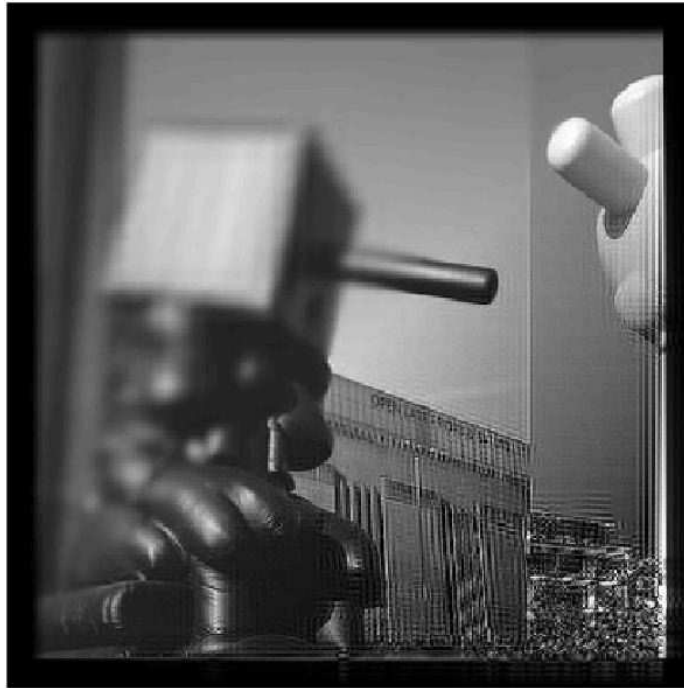


FIG. 8. Test image, with blurring in N.W., sharpening in S.E.



FIG. 9. Another test image, before selective filtering.

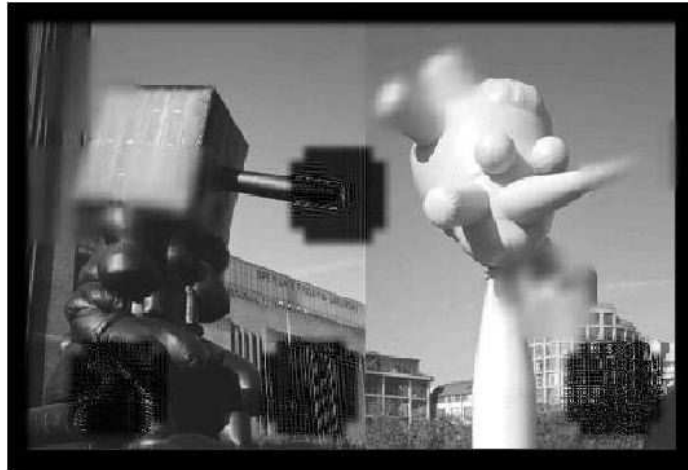


FIG. 10. Test image with selective filtering.

understanding of how they work in the more familiar situation of sounds and images.

### ACKNOWLEDGEMENTS

The authors would like to thank our funding partners, in particular CREWES, NSERC MITACS, and the POTSI sponsors.

### REFERENCES

- Feichtinger, H. G., and Strohmer, T., 1998, *Gabor Analysis and Algorithms: Theory and applications*: Birkhauser.
- Gibson, P. C., Lamoureux, M. P., and Margrave, G. F., 2003, Representation of linear operators by Gabor multipliers: CREWES Research Report, **15**.
- Grossman, J., Margrave, G. F., Lamoureux, M. P., and Aggarwala, R., 2002, Constant-Q wavelet estimation via a Gabor spectral model: Canadian Soc. Expl. Geophys. Annual Meeting, Expanded Abstracts.
- Margrave, G. F., Lamoureux, M. P., Grossman, J. P., and Iliescu, V., 2002, Gabor deconvolution of seismic data for source waveform and Q correction: 72nd Ann. Internat. Mtg. Soc. of Expl. Geophys., Expanded Abstracts, 2190–2193.